Frontiers in Heat and Mass Transfer (FHMT), 18, 18 (2022)
DOI: 10.5098/hmt.18.18

Global Digital Central
ISSN: 2151-8629

Frontiers in Heat and Mass Transfer

Available at www.ThermalFluidsCentral.org

EFFECT OF MELTING HEAT TRANSFER AND THERMAL RADIATION ON SQUEEZING FLOW OF A CASSON FLUID WITH CHEMICAL REACTION IN POROUS MEDIUM

Bhagawan Singh Yadav and Sushila Choudhary†

Department of Mathematics, University of Rajasthan, Jaipur, Rajasthan, 302004, India

ABSTRACT

The present study concentrates on squeeze MHD flow of Casson fluid between parallel plates surrounded by a porous medium. The influence of melting, viscous dissipation and thermal radiation on the heat transfer process is disclosed. The characteristics of mass transport are detected with chemical reactions. Suitable similarity transforms are used to convert the partial differential equations into a system of ordinary differential equations. The transformed equations are solved using the bvp4c matlab solver with the shooting method. Our present study concluded that fluid velocity has direct relation with melting parameter while it is reciprocally related to squeezing parameter and reverse scenario exhibited in temperature distribution. The behaviour of velocity profile, temperature profile and concentration profile of the fluid are illustrated graphically and widely discussed. Previously attempted numerical/semi-analytic approaches (RK-SM, Keller Box and OHAM) are used to validate present numerical solutions.

Keywords: *Casson fluid, Squeezing flow, Melting heat transfer, Viscous dissipation, Thermal radiation, Chemical reaction.*

1. INTRODUCTION

The squeeze flow of a non-Newtonian fluid has been soil of active research area, being the broad range of applications in engineering, industrial problems and biological processes, such as Magnetorheological and electrorheological dampers (Ahamed *et al.* (2016)), glues, tars, biological solution, polymers, compression moulding of polymers, metals and motor bearings (Wang *et al.* (2017)), etc. In the engineering area, electrorheological fluids are sometimes used to make dampers, bearings, motors, and lubrication, which involve fluid squeezing. The polymer and metal compression moulding processes (filled or unfilled) are basically based on squeeze flow. Stefan (1874) introduced experiments on squeezing flow at the outset. The distribution of radial pressure in the presence of inertia terms in squeezing film has been formulated by Jackson (1962). A squeezing film creation from the original Reynolds-Stefan equation has been studied by Moore (1965). Wang (1976) analyzed the unsteady viscous fluid lies between two parallel plates which are being squeezing or separated. In his analysis the relative normal velocity is proportional to $(1-\alpha t)^{-1/2}$. Nakamura and Sawada (1987) established the constitutive equation of a slurry which is described as a Bingham plastic fluid. The numerical investigtion of non-Newtonian fluid through an axisymmetric stenosis has been carried out by Nakamura and Sawada (1988). Tashtoush *et al.* (2001) studied the influence of viscous dissipation and axial convalution on the dynamicity of temperature, velocity and pressure. Duwairi *et al.* (2004) examined the heat transfer of the squeezed and extruded viscous fluid located between two parallel plates. The convective heat and mass transfer through a stretching sheet with chemical reaction in the presence of uniform transverse magnetic field has been explored by Afify (2004).

A numerical and analytical investigation of the heat transfer and squeezing flow between two parallel disks in the presence of electric field has been carried out by Bahadir and Abbasov (2011). The heat and mass transfer analysis of unsteady squeezing viscous fluid flow between parallel plates has been depicted by Mustafa *et al.* (2012). Khan *et al.* (2014) studied the MHD squeezing flow problem by variation of parameters method(VPM). In 2015, Huilgol get published his ideas on "Fluid Mechanics of Viscoplasticity" in the form of a book. A theoretical study of MHD flow of a Casson fluid over exponentially inclined permeable stretching surface in the presence of thermal radiation and chemical reaction has been illustrated by Reddy (2016). Khan *et al.* (2016) examined the heat transfer for a Casson fluid squeezed between parallel plates. Comparison of analytical and numerical results of MHD unsteady squeezing flow of Casson fluid passing through the porous medium has been carried out by Khan *et al.* (2016). Mabood *et al.* (2016) studied the influence of melting heat transfer and thermal radiation in porous medium with Magnetohydrodynamics on Casson fluid over a moving surface. The study of heat and mass transmission over an exponential permeable stretching surface in MHD Casson fluid has been explored by Raju *et al.* (2016) and Biswas *et al.* (2017) extended this work considering time dependent flow. Naduvinamani and Shankar (2019) demonstrated

† *Corresponding author. Email: sumathru11@gmail.com*

the analysis of heat and mass transmission of MHD squeeze Casson fluid flow between parallel plates subjected to viscous and joule dissipation effect with chemical reaction. Also compared the behavior of the squeezing flow of Casson fluid with Newtonian fluids. The influence of melting heat transfer on MHD Casson fluid flow in a porous medium passing through the stretching sheet with radiation has been illustrated by Mabood and Das (2019). Sobamowo *et al.* (2019) presented the squeezing flow of unsteady MHD Casson nanofluid between parallel plates embedded in porous medium. The heat and mass transfer peculiarity of MHD Casson fluid flow between parallel plates under the influence of thermal radiation, internal heat generation or absorption and joule dissipation effects with chemical reaction has been disclosed by Naduvinamani and Shankar (2019). Ahmad *et al.* (2020) exhibited the squeezed unsteady MHD flow of Jeffrey fluid confined between two infinite parallel plates under the influence of melting, thermal radiation and viscous dissipation effects with first order chemical reaction.

The MHD heat and mass transfer of Casson fluid flow passing through the permeable stretching sheet in the presence of chemical reaction with melting and radition effects has been studied by Ramana *et al.* (2020). Noor *et al.* (2020) exposed the MHD squeezing flow of Casson nanofluid with chemical reaction, thermal radiation and heat generation/absorption. Heat transfer in an unsteady vertical porous channel with injection/suction in the presence of heat generation has been studied by Obalalu *et al.* (2020). Obalalu *et al.* (2020) demonstrated numerical simulation of entropy generation for Casson fluid flow through permeable walls and convective heating with thermal radiation effect. Obalalu (2021) investigated the effects of variable thermophysical properties on MHD unsteady Casson fluid flow, taking into account radiation and dissipation process.

The above literature survey show the bulk of existing research on squeezing flow for Newtonian and non-Newtonian fluids. The non-Newtonian Casson fluid was also discussed with the melting phenomena. But such analysis of squeezing flow with melting heat transport for Casson fluid has not been explored yet. So, filling this vacuum in the core strategic issue, the effect of melting heat transfer on squeezing flow of a Casson fluid with thermal radiation effects in the presence of chemical reaction is discussed in this work. Using non-dimensional parameters, the governing system of partial differential equations are transformed to a system of non-linear ordinary differential equations. The transformed equations are solved numerically in MATLAB software through the bvp4c solver along with shooting technique. The effect of various parameters on velocity profile, temperature profile and concentration profile has been analysed with graphs and tables as discussed in results and disscussion section. Also, validation of numerical solutions for skin friction coeffiecient is presented via table 4, which provide a supportive hand to our used calculation model(Shooting method with bvp4c solver).

2. MATHEMATICAL FORMULATION

We consider the heat and mass transfer analysis in the unsteady, incompressible, MHD squeezing flow of a Casson fluid between two horizontal parallel plates. One plate is located at $y = 0$ and other is placed at $y = l\sqrt{1-\alpha t} = h(t)$, where l is the initial position at time $t = 0$. In case of $\alpha > 0$ the plates are squeezed until they touch each other at $t = 1/\alpha$ and when $\alpha < 0$ the plates are segregated. Also, impact of viscous dissipation is considered to investigate the production of heat due to friction caused by shear in the flow. The applied magnetic field *(B)* is acting along the vertical direction and induced magnetic field is negleted as compared to applied magnetic field, considering the small Reynolds number. The time-dependent chemical reaction is taken into consideration. Rheological conditions of Casson fluid is defined as under (Nakamura and Sawada (1987, 1988), Huilgol (2015)).

$$\tau_{ij} = \left[\mu_B + (\frac{P_y}{\sqrt{2\pi_c}})\right] 2e_{ij}, \tag{1}$$

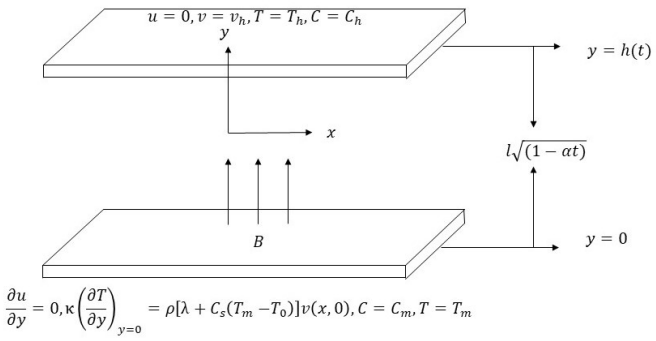

Fig. 1 Graphical representation of the flow problem

where μ_B is the Casson coefficient of viscosity, P_y is the yield stress of fluid, π_c represents product of the component of deformation rate with itself, e_{ij} is (i, j) component of the deformation rate.

$$\frac{\partial u}{\partial x} + \frac{\partial v}{\partial y} = 0\,, \tag{2}$$

$$\frac{\partial u}{\partial t} + u\frac{\partial u}{\partial x} + v\frac{\partial u}{\partial y} = \frac{-1}{\rho}\frac{\partial p}{\partial x} + \nu\left(1+\frac{1}{\beta}\right)\left(2\frac{\partial^2 u}{\partial x^2} + \frac{\partial^2 u}{\partial y^2} + \frac{\partial^2 v}{\partial x \partial y}\right) - \frac{\sigma B^2 u}{\rho} - \frac{\mu}{K\rho}\left(1+\frac{1}{\beta}\right)u\,, \tag{3}$$

$$\frac{\partial v}{\partial t} + u\frac{\partial v}{\partial x} + v\frac{\partial v}{\partial y} = \frac{-1}{\rho}\frac{\partial p}{\partial y} + \nu\left(1+\frac{1}{\beta}\right)\left(2\frac{\partial^2 v}{\partial x^2} + \frac{\partial^2 v}{\partial y^2} + \frac{\partial^2 u}{\partial x \partial y}\right) - \frac{\mu}{K\rho}\left(1+\frac{1}{\beta}\right)v\,, \tag{4}$$

$$\frac{\partial T}{\partial t} + u\frac{\partial T}{\partial x} + v\frac{\partial T}{\partial y} = \frac{\kappa}{\rho C_p}\left(\frac{\partial^2 T}{\partial x^2} + \frac{\partial^2 T}{\partial y^2}\right) + \frac{\nu}{C_p}\left(1+\frac{1}{\beta}\right)\left[2\left(\frac{\partial u}{\partial x}\right)^2 + \left(\frac{\partial u}{\partial y} + \frac{\partial v}{\partial x}\right)^2 + 2\left(\frac{\partial v}{\partial y}\right)^2\right] - \frac{1}{\rho C_p}\frac{\partial q_r}{\partial y}\,, \tag{5}$$

$$\frac{\partial C}{\partial t} + u\frac{\partial C}{\partial x} + v\frac{\partial C}{\partial y} = D\left(\frac{\partial^2 T}{\partial x^2} + \frac{\partial^2 T}{\partial y^2}\right) - K_1(t)C. \tag{6}$$

The relevant boundary conditions are

$$\begin{cases} \frac{\partial u}{\partial y} = 0,\ \kappa\left(\frac{\partial T}{\partial y}\right)_{y=0} = \rho\left[\lambda + C_s\left(T_m - T_0\right)\right]v(x,0), \\ C = C_m,\ T = T_m, \qquad at\ y = 0 \\ u = 0,\ v = v_h = \frac{dh(t)}{dt},\ T = T_h,\ C = C_h \qquad at\ y = h(t) \end{cases} \tag{7}$$

Here *u* and *v* are the velocity components in *x* and y directions, respectively, $\beta = \mu_B\frac{\sqrt{2\pi_c}}{p_y}$ is the Casson fluid parameter, ρ is fluid density, ν is kinematic viscosity, σ is the electrical conductivity of the fluid, *K* is the permeability of the medium, p is the pressure, κ is thermal conductivity, C_p is the specific heat, q_r is the radiative heat flux, D is the diffusion coefficient, $K_1(t) = \frac{K_0}{1-\alpha t}$ is the time-dependent reaction rate, λ is the latent heat of the fluid, *C* is the concentration, C_s is the heat capacity of the solid surface. The expression of q_r can be written as (Mabood *et al.* (2016)).

$$q_r = -\frac{4\sigma^*}{3\kappa^*}\left(\frac{\partial T^4}{\partial y}\right) \tag{8}$$

Here κ^* is the mean absorption coefficient and σ^* is the Stefan-Boltzmann constant and $T^4 \approx 4T_h^3 T - 3T_h^4$.

From equations [3-4] eliminating pressure terms p and using equation (2), we get

$$\frac{\partial w}{\partial t}+u\frac{\partial w}{\partial x}+v\frac{\partial w}{\partial y}=\nu\left(1+\frac{1}{\beta}\right)\left(\frac{\partial^2 w}{\partial x^2}+\frac{\partial^2 w}{\partial y^2}\right)+\frac{\sigma B^2}{\rho}\frac{\partial u}{\partial y} -\frac{\mu}{K\rho}\left(1+\frac{1}{\beta}\right)w\,, \quad (9)$$

where

$$w=\left(\frac{\partial v}{\partial x}-\frac{\partial u}{\partial y}\right) \quad (10)$$

Using equation (8) into equation (5) we get

$$\frac{\partial T}{\partial t}+u\frac{\partial T}{\partial x}+v\frac{\partial T}{\partial y}=\frac{\kappa}{\rho C_p}\left(\frac{\partial^2 T}{\partial x^2}+\frac{\partial^2 T}{\partial y^2}\right)+\frac{\nu}{C_p}\left(1+\frac{1}{\beta}\right) \left[2\left(\frac{\partial u}{\partial x}\right)^2+\left(\frac{\partial u}{\partial y}+\frac{\partial v}{\partial x}\right)^2+2\left(\frac{\partial v}{\partial y}\right)^2\right]+\frac{16\sigma^*}{3\kappa^*\rho C_p}T_h^3\frac{\partial^2 T}{\partial y^2}\,, \quad (11)$$

The similarity variables are (Mustafa *et al.*, 2012)

$$u=\frac{\alpha x}{2(1-\alpha t)}F'(\eta), \qquad v=\frac{-\alpha l}{2\sqrt{(1-\alpha t)}}F(\eta),$$

$$\theta=\frac{T-T_m}{T_h-T_m}, \qquad \phi=\frac{C-C_m}{C_h-C_m}, \quad (12)$$

where

$$\eta=\frac{y}{l\sqrt{(1-\alpha t)}}. \quad (13)$$

Now the governing equations in the view of equations (12) and (13), take the forms

$$\left(1+\frac{1}{\beta}\right)F''''(\eta)-\mathrm{S}\left[\eta F'''(\eta)+3F''(\eta)+F'(\eta)F''(\eta) -F(\eta)F'''(\eta)\right]-\mathrm{Mg}F''(\eta)-\mathrm{Mp}\left(1+\frac{1}{\beta}\right)F''(\eta)=0\,, \quad (14)$$

$$\left(\frac{4}{3}\mathrm{Ra}+1\right)\theta''(\eta)+\mathrm{Pr\ S}\left[F(\eta)\theta'(\eta)-\eta\theta'(\eta)\right]+\mathrm{PrEc} \left(1+\frac{1}{\beta}\right)\left[(F''(\eta))^2+4\delta^2(F'(\eta))^2\right]=0\,, \quad (15)$$

$$\phi''(\eta)-\mathrm{S\ Sc}\left(\eta\phi'(\eta)-F(\eta)\phi'(\eta)\right)-2\mathrm{S\ Sc}\,\gamma\phi(\eta)=0\,, \quad (16)$$

and the corresponding boundary conditions are

$$\begin{cases} F''(\eta)=0,\ \mathrm{Me}\ \theta'(\eta)+\mathrm{Pr\ S}\ F(\eta)=0, \\ \theta(\eta)=0,\ \phi(\eta)=0, \quad at \quad \eta=0; \\ F'(\eta)=0,\ F(\eta)=1,\ \theta(\eta)=1,\ \phi(\eta)=1 \quad at \quad \eta=1, \end{cases} \quad (17)$$

where $S=\frac{\alpha l^2}{2\nu}$, $Mg=\frac{\sigma\beta^2 l^2}{\rho\nu}(1-\alpha t)$, $Mp=\frac{\mu l^2}{\rho K\nu}(1-\alpha t)$, Pr=$\frac{\mu C_p}{\kappa}$, $Ec=\frac{1}{C_p(T_h-T_m)}\left(\frac{\alpha x}{2(1-\alpha t)}\right)^2$, $Ra=\frac{4\sigma^* T_H^3}{\kappa\kappa^*}$, $Sc=\frac{\nu}{D}$, $\gamma=\frac{K_0}{\alpha}$, and $Me=\frac{(T_h-T_m)C_p}{[\lambda+C_s(T_h-T_0)]}$ represent squeeze number, MHD parameter, porous medium parameter, Prandtl number, Eckert number, radiation parameter, Schmidt number, chemical reaction parameter and melting parameter, respectively and $\delta=\frac{l}{x}(1-\alpha t)^{1/2}$.

The surface shear stress, surface heat flux and surface mass flux, respectively are given by (Naduvinamani and Shankar (2019))

$$\tau_w=\mu\left(1+\frac{1}{\beta}\right)\left(\frac{\partial u}{\partial y}\right)_{y=h(t)}, \quad (18)$$

$$q_w=-\kappa\left(\frac{\partial T}{\partial y}\right)_{y=h(t)}+q_r, \quad (19)$$

$$q_s=-D\left(\frac{\partial C}{\partial y}\right)_{y=h(t)}. \quad (20)$$

The skin friction coefficient, local Nusselt number and Sherwood number, respectively, are defined as

$$C_f=\frac{\tau_w}{\rho v_h^2} \Rightarrow \frac{l^2}{x^2}(1-\alpha t)Re_x C_f=\left(1+\frac{1}{\beta}\right)F''(1)\,, \quad (21)$$

$$Nu_x=\frac{xq_w}{\kappa(T_h-T_m)} \Rightarrow (1-\alpha t)^{1/2}Nu_x=-(1+\frac{4}{3}Ra)\theta'(1)\,, \quad (22)$$

and

$$Sh=\frac{lq_s}{D(C_h-C_m)} \Rightarrow (1-\alpha t)^{1/2}Sh=-\phi'(1)\,, \quad (23)$$

where $Re_x=\frac{xv_h}{\nu}$ is the local Reynolds number based on the Squeezing velocity v_h.

3. METHOD OF SOLUTION

It is not easy to find the exact solution of the above system of nonlinear ordinary differential equations [14-16]. So in this situation, we are interested to find approximate solution of the problem using numerical methods. Here the nonlinear boundary layer equations (14), (15) and (16) with the boundary condition (17) are solved by bvp4c Matlab solver along with shooting technique. Here we have obtained a non-dimensional mathematical model in the form of ODE system having prescribed boundary condition at two points i.e. $\eta=0$ and $\eta=1$. We know that it is much easier to solve an IVP (Initial Value Problem) than a BVP (Boundary Value Problem). Shooting method is a widely known tool which is used to convert an IVP to BVP. It is purely based on hit & trail procedure but have less computational cost. For the initial value problem, the shooting technique takes use of the speed and adaptability of approaches.
Let $F=f_1$, $F'=f_2$, $F''=f_3$, $F'''=f_4$, $\theta=f_5$, $\theta'=f_6$, $\phi=f_7$, $\phi'=f_8$, then we get following system of first order differential equations:

$$f_1'=f_2,$$
$$f_2'=f_3,$$
$$f_3'=f_4,$$

$$f_4'=\frac{S}{1+1/\beta}\left[\eta f_4+3f_3+f_2f_3-f_1f_4\right]+\frac{(Mgf_3+Mpf_3)}{1+1/\beta},$$

$$f_5'=f_6,$$

$$f_6'=\frac{-PrS\left[f_1f_6+\eta f_6\right]+PrEc(1+1/\beta)\left[f_3^2+4\delta^2 f_2^2\right]}{(\frac{4}{3}Ra+1)},$$

$$f_7'=f_8,$$

$$f_8'=SSc\left(\eta f_8-f_1f_8\right)+2SSc\sigma f_8-f_1f_7,$$

subject to the following boundary conditions:

$$\begin{cases} f_3=0,\ f_5=0,\ Mef_6+SPrf_1=0,\ f_7=0 \quad at \quad \eta=0; \\ f_1=1,\ f_2=0,\ f_5=1,\ f_7=1 \quad at \quad \eta=1. \end{cases}$$

We have used shooting procedure to find the initial guesses for absent values at $\eta=0$ and converted the above system into an IVP. By using bvp4c solver, we find the values of $F''(\eta)$, $\theta'(\eta)$ and $\phi'(\eta)$ at η=1, for different values of physical parameters. The bvp4c method in MATLAB is a convenient and easy-to-use, that can solve rather complex issues. For solving nonlinear system of equations, this algorithm uses an iteration structure. bvp4c is a finite-difference code that implements the Lobatto IIIa formula in three stages. Also, effects of various physical parameters on velocity, temprature and concentration profiles are illustrated graphically by using this algorithm.

Global Digital Central
ISSN: 2151-8629

4. RESULTS AND DISCUSSION

This section highlights the influence of emerging parameters on the boundary layer flow, melting heat transfer and concentration of Casson fluid due to a squeezing flow. We shall discuss the effect of various parameters like melting parameter (Me), squeezing number (S), MHD parameter (Mg),Porous medium parameter (Mp), Prandtl number (Pr), Eckert number (Ec), Radiation parameter (Ra), Schmidt number (Sc), Casson fluid parameter (β) and chemical reaction parameter (γ) on the velocity profile, temperature profile and concentration profile through the graphs and tables. These effects are displayed from Fig. 2 to Fig. 18. The default values of the parameters are set as $S = 0.2, Me = 0.5, \beta = 0.4$, Pr=3, $Mg = 0.7, Mp = 0.6, Ec = 0.01, Ra = 0.5, Sc = 1.2, \gamma = 0.1, \delta = 0.1$, unless otherwise specified. The impact of squeezing number on velocity profile is illustrated in Fig. 2 and 3. Fig. 2 is for $Me > 0$ and Fig. 3 is for $Me = 0$, while other parameters are constant. Fig. 2 represents that the velocity profile decreases with increasing values of squeezing number. Fig. 3 represents that the velocity profile decreases for $\eta < 0.45$ and there is change in the behaviour of velocity profile when $0.45 < \eta < 1$. The effect of squeezing number on the temperature profile is described in Fig. 4.

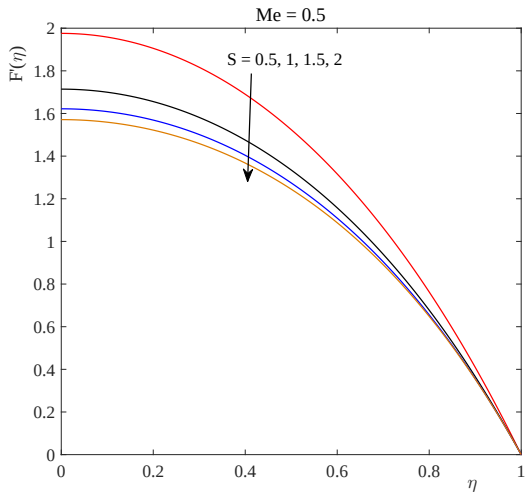

Fig. 2 Influence of S on $F'(\eta)$ when $Me > 0$

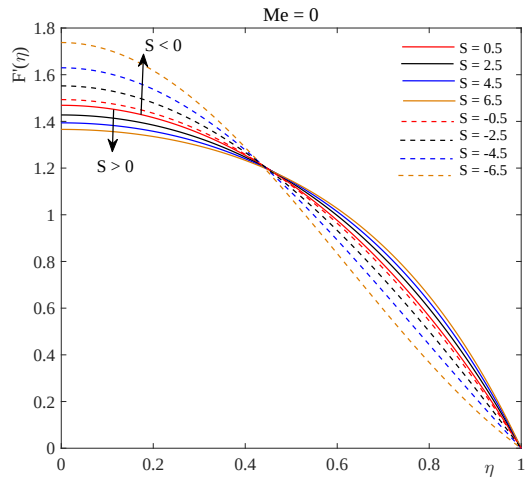

Fig. 3 Influence of S on $F'(\eta)$ when $Me = 0$

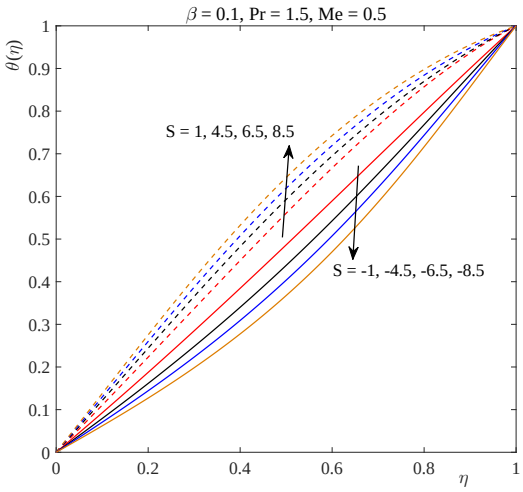

Fig. 4 Influence of S on $\theta(\eta)$

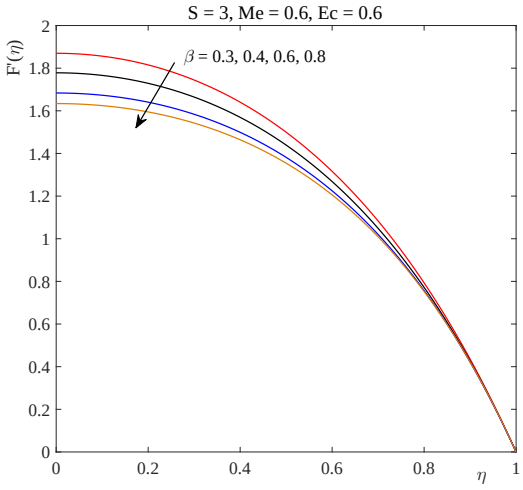

Fig. 5 Influence of β on $F'(\eta)$ when $Me > 0$.

Fig. 4 clearly shows that the temperture profile is increased by an increase in the squeezing number.

The impact of Casson fluid parameter on velocity profile is shown in Figs. $[5-7]$. From Fig. 5, when $S > 0$ and $Me > 0$, it is clear that the velocity profile decreases with increasing values of Casson fluid parameter. In Fig. 6, we consider the case when $Me = 0$ and $S < 0$, and notice that there exist a critical value $\eta = 0.425$ such that the velocity profile increases for $\eta < 0.425$ and decreases for $\eta > 0.425$. From Fig. 7, it is oserved that when $Me = 0$ and $S > 0$, there exist a critical value $\eta = 0.455$ such that the velocity profile decreases for $\eta < 0.455$ and increases for $\eta > 0.455$. The effect of the Casson fluid parameter on the temperature profile is displayed in Fig. 8. It is clear from Fig. 8 that as the value of Casson fluid parameter increases, the temperature profile decreases.

Fig. 9 and Fig. 10 demonstrate the influence of melting parameter on velocity profile and temperature profile, respectively. It is apparent that, with increasing values of melting parameter, the velocity profile increases and temperature profile diminishes. A larger melting value improves the thickness of the momentum boundary layer. In terms of physics, an increase in Me will enhance the intensity of melting, resulting in more heat transfer from the heated fluid to the melting surface. As a re-

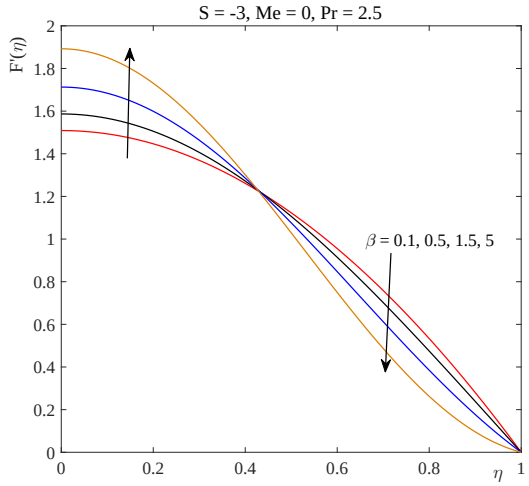

Fig. 6 Influence of β on $F'(\eta)$ when $Me = 0$ and $S < 0$

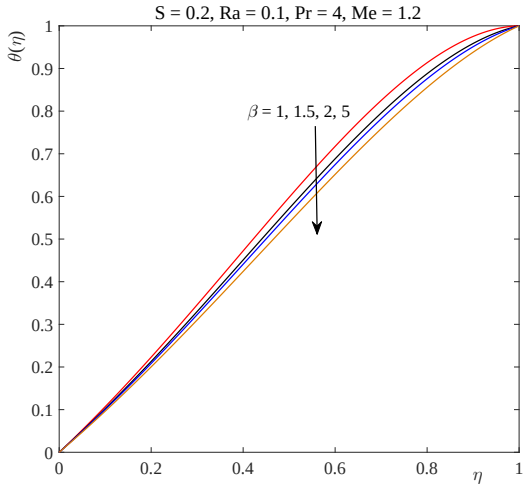

Fig. 8 Influence of β on $\theta(\eta)$.

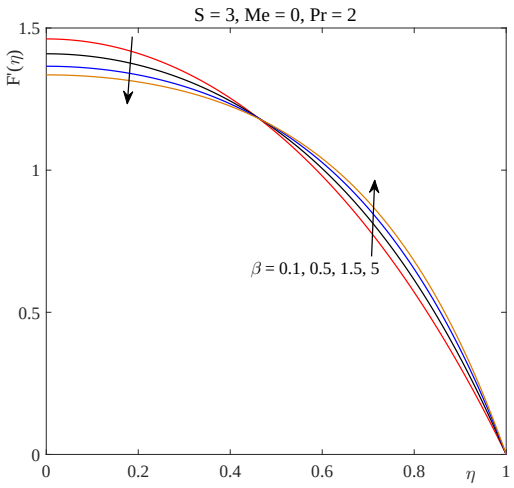

Fig. 7 Influence of β on $F'(\eta)$ when $Me = 0$ and $S > 0$

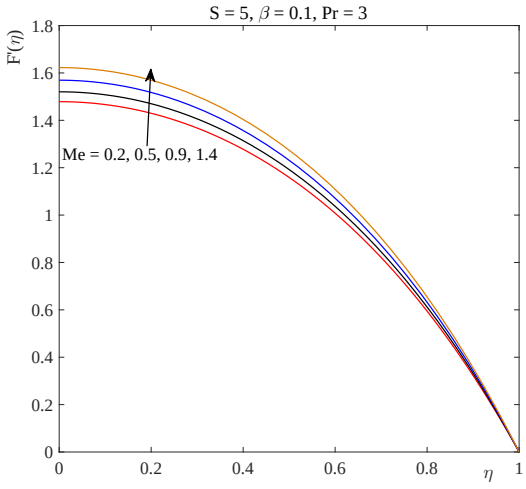

Fig. 9 Influence of Me on $F'(\eta)$.

sult of this, there is more convection flow, which increases fluid velocity. The melting parameter, as can be seen in Fig. 10, reduces the temperature distribution. These findings make sense physically and hence, the melting process can act as a blowing boundary condition at the extending surface. Additionally, by increasing the values of the melting parameter, the gap between the fluid ambient temperature and the temperature of the melting surface grows, resulting in a decrease in the fluid temperature. As a result, with increasing melting parameter (Me), the thermal boundary layer thickness rises. Fig. 11 indicates the effect of MHD parameter on the velocity profile. It is ascertained that, with increasing MHD parameter, the velocity profile decreases for $0 < \eta < 0.457$ and increases for $0.457 < \eta < 1$. This means that the transverse magnetic field opposes transport phenomena because increasing (Mg) increases the Lorentz force, which opposes the transport process. The Lorentz force increases as (Mg) increases owing to the interplay of electric and magnetic fields in the electrically conducting fluid. Fig.12 demonstrates the influence of porous medium parameter on the velocity profile. It is noticed that, with increasing values of porous medium parameter, the velocity profile decreases for $0 < \eta < 0.455$ and suddenly the behaviour of velocity profile is changed after $\eta = 0.455$. Fig. 13 and Fig. 14 display the effect of Prandtl number on the velocity profile and temperature profile, respectively. The inference is taken from Fig. 13 that the increasing value of the prandtl number decreases the velocity profile. From Fig. 14 we note that the temperature profile increases with incresing values of Prandtl number.

The fluctuation of Eckert number on temperature profile is conveyed in Fig. 15. From Fig. 15, it is clear that the temperature profile increases with increasing value of Eckert number. This is because the existence of frictional forces in the fluid causes heat energy to be emitted into the fluid, amplifying the temperature field in the flow zone. Furthermore, the existence of viscous dissipation raises the temperature field. Since Ec is explicitly mentioned in the temperature equation, the temperature field may be readily controlled by adjusting Ec. The influence of the radiation parameter on the temperature profile is included in Fig. 16. This is appeared that the temperature profile decreases with increasing value of radiation parameter. Reasons behind this trend is that radiation has the effect of slowing the flow of energy into the fluid, lowering its temperature.

Fig. 17 illustrates the physical characteristics of Schmidt number on the curve of concentration. Reduction is observed in the area of concentration with a growing Schmidt number. For a greater Schmidt number, mass diffusivity declines. This is owing to the fact that increasing Sc

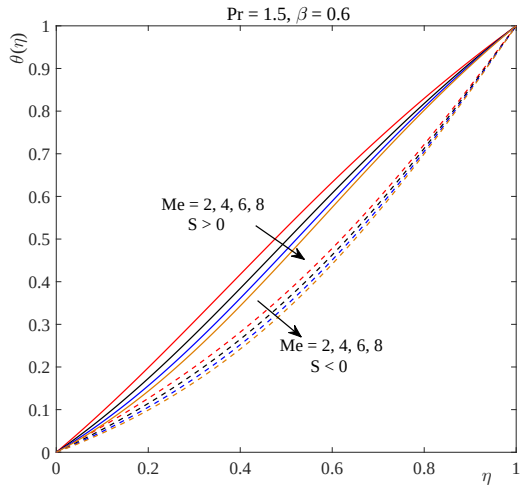

Fig. 10 Influence of *Me* on $\theta(\eta)$.

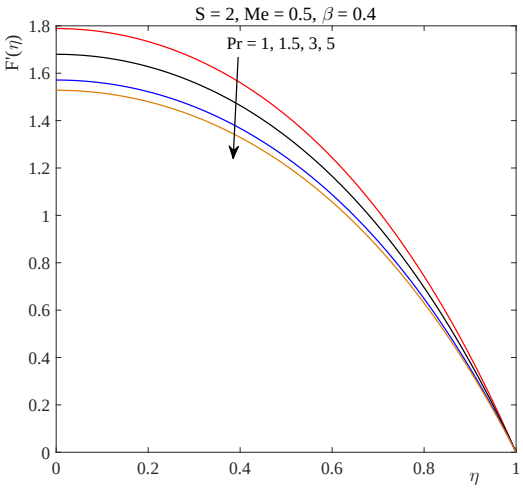

Fig. 13 Influence of Pr on $F'(\eta)$.

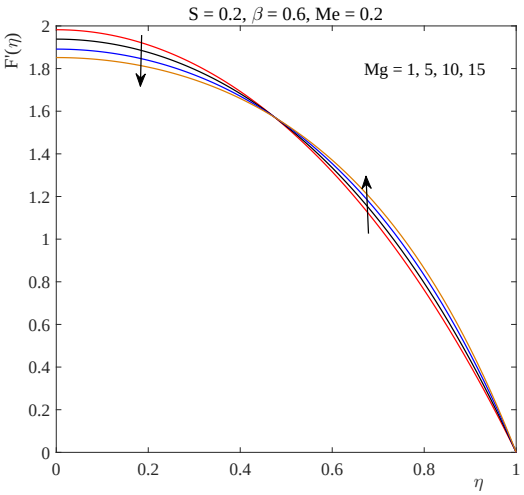

Fig. 11 Influence of *Mg* on $F'(\eta)$.

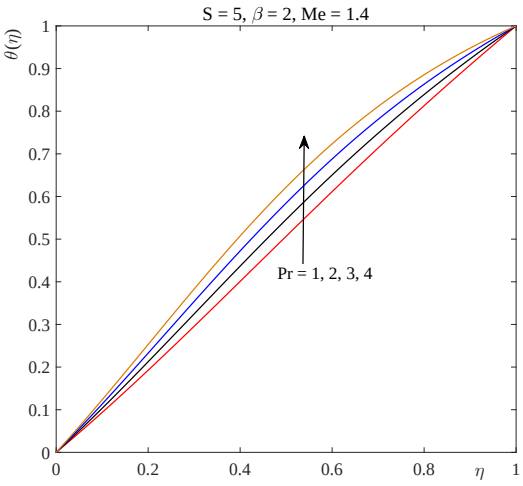

Fig. 14 Influence of Pr on $\theta(\eta)$.

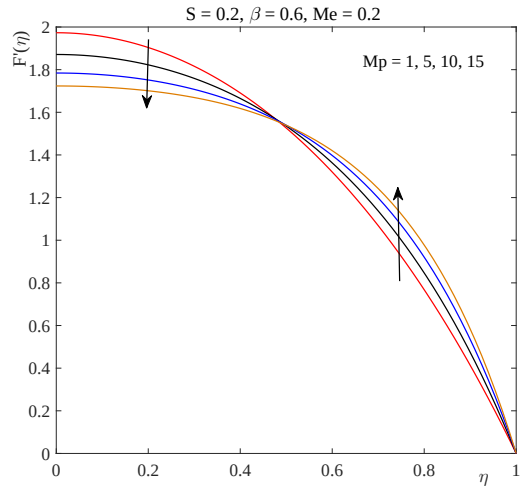

Fig. 12 Influence of *Mp* on $F'(\eta)$.

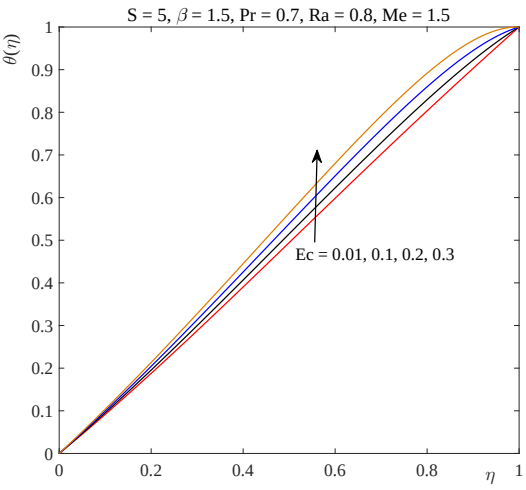

Fig. 15 Influence of *Ec* on $\theta(\eta)$.

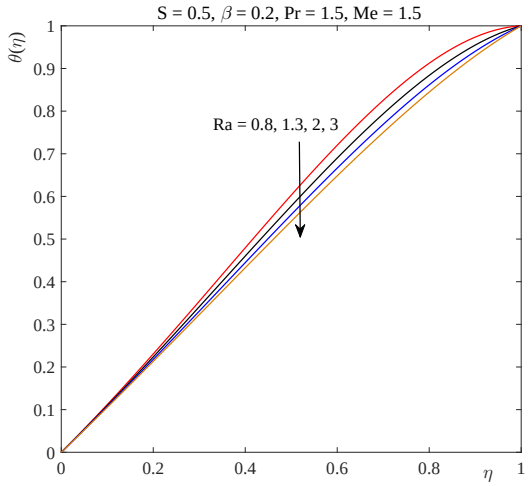

Fig. 16 Influence of Ra on $\theta(\eta)$

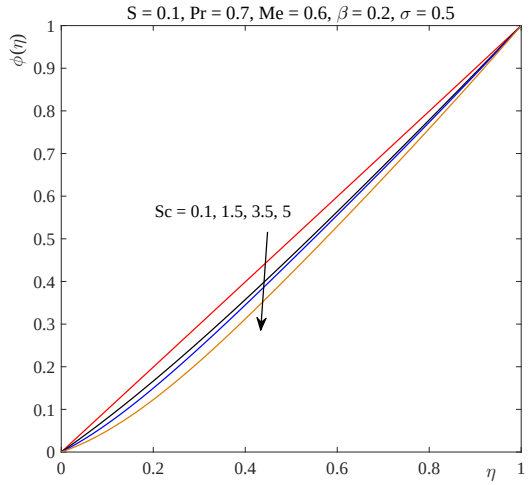

Fig. 17 Influence of Sc on $\phi(\eta)$

decreases the molecular diffusion coefficient, reducing the concentration field in the flow region. The effect of a chemical reaction parameter on the concentration profile is shown in Fig. 18. From the Fig. 18, we observed that the concentration profile decreases with increasing values of chemical reaction parameter. Table 1, table 2 and table 3 present the numerical values of the skin friction coefficient, Nusselt number and Sherwood number, respectively along with the varied values of S, β, Me, Pr, Mg, Mp, Ec, Ra, Sc, and γ.

5. CONCLUSIONS

The present work, we have investigated the squeezing MHD flow of a Casson fluid between parallel plates situated in porous medium. The heat transfer is featured with melting heat transfer, viscous dissipation and thermal radiation. The mass transport is characterized by first order chemical reaction. The bvp4c solver is used to solve the transformed governing equations. In table 4, the numerical solutions for skin friction coefficient are validated with prior published research, and both findings show great agreement. When the plates move apart ($S > 0$), the fluid velocity decreases, and it increases when the plates move closer ($S<0$). The increase in the Mg and Mp refers to a decrease in the velocity profile near

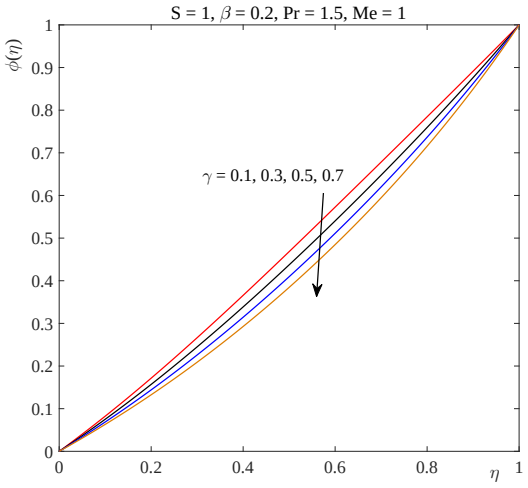

Fig. 18 Influence of γ on $\phi(\eta)$

Table 1 Numerical values for skin friction coefficient at the upper plate.

S	β	Me	Pr	Mg	Mp	$F''(1)$
0.5	0.4	0.5	3	0.7	0.6	-4.3989
1						-3.9546
2						-3.8705
6.5	0.4	0	3	0.7	0.6	-4.2113
2.5						-3.6055
0.5						-3.2520
-0.5						-3.0577
-2.5						-2.6227
-6.5						-1.4405
3	0.1	0	2	0.7	0.6	-3.3113
	0.5					-3.7091
	5					-4.5596
-3	0.1	0	2.5	0.7	0.6	-2.9369
	0.5					-2.3835
	1.5					-1.5892
	5					-0.5743
3	0.3	0.6	3	0.7	0.6	-3.8911
	0.4					-3.9993
	0.6					-4.1692
	0.8					-4.2963
5	0.1	0.2	3	0.7	0.6	-3.5023
		0.5				-3.6060
		0.9				-3.7283
		1.4				-3.8616
2	0.4	0.5	1	0.7	0.6	-4.4443
			1.5			-4.1562
			3			-3.8705
			5			-3.7575
0.2	0.6	0.2	3	1	0.6	-4.3802
				5		-4.7362
				10		-5.1477
				15		-5.5284
0.2	0.6	0.2	3	0.7	1	-4.4505
					5	-5.3364
					10	-6.2667
					15	-7.0672

Table 2 Numerical values for Nusselt number at the upper plate.

S	β	Me	Pr	Ec	Ra	$-\theta'(1)$
1	0.1	0.5	1.5	0.01	0.5	-0.5528
4.5						-0.5257
6.5						-0.4490
8.5						-0.3762
-4.5						-1.1224
-6.5						-1.2642
-8.5						-1.4230
0.2	1	1.2	4	0.01	0.1	-0.0229
	1.5					-0.2339
	2					-0.3305
	5					-0.4931
5	0.6	2	1.5	0.01	0.5	-0.7816
		4				-0.8272
		6				-0.8590
		8				-0.8829
5	2	1.4	1	0.01	0.5	-0.8985
			2			-0.7424
			3			-0.5995
			4			-0.4699
5	1.5	1.5	0.7	0.01	0.8	-0.9576
				0.1		-0.6660
				0.2		-0.3260
0.5	0.2	1.5	1.5	0.01	0.8	-0.0542
					1.3	-0.2959
					2	-0.4832
					3	-0.6262

Table 3 Numerical values for Sherwood number at the upper plate.

S	β	Me	Pr	Sc	γ	$-\phi'(1)$
0.1	0.2	0.6	0.7	0.1	0.5	-1.0044
				1.5		-1.1191
				3.5		-1.1635
				5		-1.2513
1	0.2	1	1.5	1.5	0.1	-1.0976
					0.3	-1.2762
					0.5	-1.4435
					0.7	-1.6009

the lower stationary plate for $0 < \eta < 0.455$ and an increase in velocity profile away from the lower plate for $0.455 < \eta < 1$. The Nusselt number is observed to grow with *Me*, *Ra*, and β, while it decreases with *S*, *Pr*, and *Ec*. With increasing values of *Me* and *Mp*, the skin friction coefficient drops, whereas S and Pr have the opposite effect. An increase in the melting parameter causes an increase in the velocity profile and decrease in the temperature profile.

The melting event operates as a blown boundary condition at the surface. As a result of the increased severity of melting (as *Me* increases), the boundary layer thickens. The concentration field is significantly influenced by higher values of mass diffusivity and the Squeezing number. By enhancing the chemical reaction, the concentration profiles are reduced.

The presented analysis might be expanded to investigate the situation of non-Newtonian fluids and nanofluids on unsteady squeezing flow with melting phenomena. When the wall boundary conditions (stick, slip, or partial slip) calculated with high precision, squeeze flow data becomes much more valuable. With slip conditions, we may expand our work.

Table 4 Comparison of $-F''(1)$ for different values of(S) when $\beta \to \infty$, $Pr = Ec = Sc = 1$, $\delta = 0.1$, $Mg = Mp = Ra = Me = \sigma = 0$.

S	Naduvvinamani and Shanka(2019) RK-SM	Noor *et al.* (2020) Keller Box	Obalalu (2021) OHAM	Present results bvp4c-SM
-1.0	2.1700	2.1702	2.1700	2.1701
-0.5	2.6140	2.6175	2.6140	2.6174
0.01	3.0071	3.0072	3.0071	3.0071
0.5	3.3364	3.3365	3.3364	3.3364
2.0	4.1673	4.1674	4.1673	4.1674

ACKNOWLEDGEMENTS

The authors are thankful to University of Rajasthan, Jaipur for providing research facilities.

NOMENCLATURE

C_p	Specific heat (J/kg · K)
h	height (m)
k	thermal conductivity (W/m · K)
P	pressure (Pa)
ν	kinematic viscosity (m^2/s)
K	permeability of the medium (m^2)
D	diffusion coefficient (m^2/s)
t	time (s)
S	Squeezing number
T	temperature (K)
u	velocity in x direction (m/s)
v	velocity in y direction (m/s)
x, y	dimensional coordinate (m)
C	concentration (mol/m^3)
Pr	Prandtl number
Ec	Eckert number
Ra	radiation coefficient
q_r	Radiative heat flux (W/m)
Greek Symbols	
ρ	density (kg/m^3)
σ^*	Stefan-Boltzmann constant (W/m^2 · K^4)
Subscripts	
h	height
m	melting surface

REFERENCES

Afify, A.A., 2004, "MHD free convective flow and mass transfer over a stretching sheet with chemical reaction," *Heat and Mass Transfer*, **40**, 495-500.
https://doi.org/10.1007/s00231-003-0486-0

Ahamed, R., Ferdaus, M.M. and Li, Y., 2016, "Advancement in energy harvesting magneto-rheological fluid damper: A review," *Korea-Australia Rheology Journal*, **28**, 355-379.
https://doi.org/10.1007/s13367-016-0035-2

Ahmad, S., Farooq, M., Rizwan, M., Ahmad, B. and Rehman, S.U., 2020, "Melting phenomenon in a squeezed rheology of reactive rate type fluid," *Frontiers in Physics*, **8**, 108.
https://doi.org/10.3389/fphy.2020.00108

Bahadir, A.R. and Abbasov, T., 2011, "A numerical approach to

hydromagnetic squeezed flow and heat transfer between two parallel disks," *Industrial Lubrication and Tribology*, **63**, 63-71.
https://doi.org/10.1108/00368791111112171

Biswas, R., Mondal, M., Sarkar D.R. and Ahmmed, S.F., 2017, "Effects of radiation and chemical reaction on MHD unsteady heat and mass transfer of Casson fluid flow past a vertical plate," *Journal of Advances in Mathematics and Computer Science*, **23**(2), 1-16.
https://doi.org/10.9734/JAMCS/2017/34292

Casson, N., 1959, "A flow equation for pigment-oil suspension of the printing ink-type," *In: Rheology of disperse systems. Pergamon, London,* 84-104.

Duwairi, H.M., Tashtoush, B. and Damseh, R.A., 2004, "On heat transfer effects of a viscous fluid squeezed and extruded between two parallel plates," *Heat Mass Transfer*, **41**, 112-117.
https://doi.org/10.1007/s00231-004-0525-5

Huilgol, R.R., 2015, "Fluid mechanics of viscoplasticity," *Springer, Berlin*.

Jackson, J.D., 1962, "A study of squeezing flow," *Applied Science Research*, **11**, 148-152.
https://doi.org/10.1007/BF03184719

Khan, U., Ahmed, N., Zaidi, Z.A., Asadullah, M. and Mohyud-Din, S.T., 2014, "MHD squeezing flow between two infinite plates," *Ain Shams Engineering Journal*, **5**, 187-192.
https://doi.org/10.1016/j.asej.2013.09.007

Khan, U., Khan, S.I., Ahmed, N., Bano, S., Mohyud-Din, S.T., 2016, "Heat transfer analysis for squeezing flow of a Casson fluid between parallel plates," *Engineering Physics and Mathematics*, **7**, 497-504.
https://doi.org/10.1016/j.asej.2015.02.009

Khan, H., Qayyum, M., Khan, O. and Ali, M., 2016, "Unsteady flow of Casson fluid with Magnetohydrodynamic effect and passing through porous medium," *Mathematical Problems in Engineering*, ID(4293721).
https://doi.org/10.1155/2016/4293721

Moore, D.F., 1965, "A review of squeeze films," *Wear*, **8**, 245-263.
https://doi.org/10.1016/0043-1648(65)90001-3

Mustafa, M., Hayat, T. and Obaidat, S., 2012, "On heat and mass transfer in the unsteady squeezing flow between parallel plates," *Meccanica*, **47**, 1581-1589.
https://doi.org/10.1007/s11012-012-9536-3

Mabood, F., Abdel-Rahman, R.G. and Lorenzini, G., 2016, "Effect of melting heat transfer and thermal radiation on Casson fluid flow in porous medium over moving surface with megnetohydrodynamics," *Journal of Engineering Thermophysics*, **25**, 536-547.
https://doi.org/10.1134/S1810232816040111

Mabood, F. and Das, K., 2019, "Outlining the impact of melting on MHD Casson fluid flow past a stretching sheet in a porous medium with radiation," *Elsevier*, **5**, e01216.
https://doi.org/10.1016/j.heliyon.2019.e01216

Nakamura, M. and Sawada, T., 1987, "Numerical study on the laminar pulsatile flow of slurries," *Journal Non-Newton Fluid Mech*, **22**, 191-206.
https://doi.org/10.1016/0377-0257(87)80035-6

Nakamura, M. and Sawada, T., 1988, "Numerical study on the flow of a Non-Newtonian fluid through an axisymmetric stenosis," *Journal Biomech Engineering*, **110**, 137-143.
https://doi.org/10.1115/1.3108418

Naduvinamani, N.B. and Shankar, U., 2019, "Analysis of heat and mass transfer in squeezing flow of Casson fluid with Magneto-Hydrodynamic effect," *Journal of Nanofluids*, **8**, 767-780.
https://doi.org/10.1166/jon.2019.1631

Naduvinamani, N.B. and Shankar U., 2019, "Radiative squeezing flow of unsteady magneto-hydrodynamic Casson fluid between two parallel plates," *Journal of Central South University*, **26**(5), 1184-1204.
https://doi.org/10.1007/s11771-019-4080-0

Noor, N.A.M., Shafie, S. and Admon, M.A., 2020, "MHD squeezing flow of Casson nanofluid with chemical reaction, thermal radiation and heat generation/absorption," *Journal of Advanced Research in Fluid Mechanics and Thermal Sciences*, **68**(2), 94-111.
https://www.akademiabaru.com/submit/index.php/arfmts/article/view/2876

Obalalu. A.M., Ajala, A.O., Akindele, A.O., Oladapo, O.A., Adepoju, O. and Jimoh, M.O., 2021, "Unsteady squeezed flow and heat transfer of dissipative casson fluid using optimal homotopy analysis method: An application of solar radiation," *Partial Differential Equations in Applied Mathematics*, **4**, 100146(1-11).
https://doi.org/10.1016/j.padiff.2021.100146

Obalalu. A.M., 2021, "Heat and mass transfer in an unsteady squeezed Casson fluid flow with novel thermophysical properties: Analytical and numerical solution," *Heat Transfer*, 1-24.
https://doi.org/10.1002/htj.22263

Obalalu. A.M., Wahaab, F.A. and Adebayo, L.L., 2020, "Heat transfer in an unsteady vertical porous channel with injection/suction in the presence of heat generation," *Journal of Taibah University for Science*, **14**, 541-548.
https://doi.org/10.1080/16583655.2020.1748844

Obalalu. A.M., Wahaab, F.A., Kazeem, I., Abdulrazaq, A., Ajala, O.A., Oluwaseyi, A. and Adebayo, L.L., 2020, "Numerical simulation of entropy generation for Casson fluid flow through permeable walls and convective heating with thermal radiation effect," *Journal of Serbian Society for Computational Mechanics*, **14**, 503-519.
Https://10.24874/jsscm.2020.14.02.10.

Reddy, P.B.A., 2016, "Magnetohydrodynamic flow of a Casson fluid over an exponentially inclined permeable stretching surface with thermal radiation and chemical reaction," *Ain Shams Engineering Journal*, **7**, 593-602.
https://doi.org/10.1016/j.asej.2015.12.010

Raju, C.S.K., Sandeep, N., Sugunamma, V., Babu, M.J. and Reddy, J.V.R., 2016, "Heat and mass transfer in magnetohydrodynamic Casson fluid over an exponentially permeable stretching surface," *Engineering Science and Technology, an International Journal*, **19**, 45-52.
https://doi.org/10.1016/j.jestch.2015.05.010

Ramana, R.M., Kumar, J.G. and Raju, K.V., 2020, "Melting and Radiation effects on MHD heat and mass transfer of Casson fluid flow

past a permeable stretching sheet in the presence of chemical reaction," *AIP Conference Proceedings*, **2246**, 1-15.
https://doi.org/10.1063/5.0014732

Sobamowo, G., Jayesimi, L., Oke, D., Yinusa, A. and Adedibu, O., 2019, "Unsteady Casson nanofluid squeezing flow between two parallel plates embedded in a porous medium under the influence of magnetic field," *Open Journal of Mathematical Sciences*, **3**, 59-73.
https://doi.org/10.30538/oms2019.0049

Stefan, M.J., 1874, "Versuch Uber die scheinbare adhesion, Sitzungsberichte der Akademie der Wissenschaften in Wien," *Mathematik-Naturwissen*, **69**, 713-721.

Tashtoush, B., Tahat, M. and Probert, S.D., 2001, "Heat transfer and radial flows via a viscous fluid squeezed between two parallel disks," *Applied Energy*, **68**, 275-288.
https://doi.org/10.1016/S0306-2619(00)00058-1

Wang, C., 1976, "The squeezing of a fluid between two plates," *Journal of Applied Mechanics*, 579-583.
https://doi.org/10.1115/1.3423935

Wang, F., Ma, Q., Meng, W. and Han, Z., 2017, "Experimental study on the heat transfer behavior and contact pressure at the casting-mold interface in squeeze casting of aluminum alloy," *International Journal of Heat and Mass Transfer*, **112**, 1032-1043.
https://doi.org/10.1016/j.ijheatmasstransfer.2017.05.051